Intersubband transitions under strong screening effect of free carriers in the step doped InGaN/GaN Quantum Well

H. R. ALAEI* [a], R. RIEDEL[b], M. YOUNESI[c]
[a]*Department of Physics, Varamin-Pishva Branch, Islamic Azad University, Varamin, Iran.*
[b]*Department of Material Science, Darmstadt University of technology, Darmstadt, Germany.*
[c] *Department of Physics, Vali-e-Asr University* of Rafsanjan, Rafsanjan, Iran

We report on the intersubband transitions at different temperatures in the InGaN/GaN Quantum Well (QW) where they have two couple thick layers with step doping around their active region. These couple step doped layers by strong screening effect of free carriers can reduce the Quantum Confined Stark Effect (QCSE) induced by strain in the QW then blue shifts as large as 70 meV for intersubband transitions is observed at room temperature. The such improvement in optical property is attributed to an increase in the injection of electrons from Si step-doped GaN barrier layers into the well also increase in the hole accumulation due to higher valance band offset of barriers. In theory, for subband calculations we solved Schrödinger-Poisson equations self-consistently by numerov method where the Exchange–correlation, Hartree interaction and internal electric fields were considered for accurate subbands calculation.

(Received July 29, 2011; accepted January 22, 2014)

Keywords: Intersubband, Transition, Quantum Well, InGaN/GaN, Self-consistent, Photoluminescence

1. Introduction

Recent dramatic advances in nitride semiconductors, especially in GaN and its different alloys have led to high performance of new optoelectronic and electronic devices such as light emitting diodes and high temperature and high frequency field effect transistors [1-3]. Further progress in the experimental field is also expected through identifying and controlling the properties that influence the electronic band structure and thermal performance of these devices [4-6].

However, successful design of advanced nitride semiconductor devices requires critical analysis of sub-band structures by considering the influence of related material parameters such as internal electric field (the piezoelectric and spontaneous polarization fields) in the varying temperature environment where the numerous experimental investigations revealed these fields are the most important challenges in these devices and many effort have done to improve their performance [7]. In this manner a delta doping process has recently been shown to improve the performance of III-V devices. However, the effect of the position of delta -doped layer within the barrier layer of the QW structure on the efficiency of electron injection on the carrier confinement is not clearly understood. When the Si delta-doped layer was very close to the QW layer, the potential well of the Si delta-doped layer overlapped with QW potential, reducing photoluminescence intensity. When the Si delta-doped layer was very far away from the QW layer, carrier injection from the Si delta-doped layer into the QW layer was not observed [8,9].

Here, we report on intersubband transitions under strong screening effect of free carriers on piezoelectric field in step doped InGaN/InGaN QW. Then after introducing the sample structure as a novel structure (included two couple layers; p++/p+ and n/n+ around its active region) and reporting some obtained experimental results, we will proceed by reporting the computational results obtained from self-consistent numerical method in a uniform mesh size of $In_{0.05}Ga_{0.95}N$/GaN QW. The advantage of this numerical method lies on reducing the computational time and its efficiency in finding sub-band energies that extend over relatively large spatial areas for InGaN/GaN QW structures [10, 11]. In this respect, we consider the internal electric fields (piezoelectric and spontaneous polarization fields) as well as exchange–correlation and Hartree interaction for the calculation of sub-band energy [12].

2. Sample structure and its optical properties

Experimental results have obtained from $In_{0.05}Ga_{0.95}N$/GaN QW sample, grown by Low-Pressure Metal Organic Chemical Vapor Deposition (Lp-MOCVD). The (0001) sapphire substrate was initially treated with H_2 at a temperature of 1050 °C, followed by the growth of a highly doped n-type 1-μm-thick low-temperature GaN layer at 1100 °C. After a high-temperature annealing of this layer, a 1.5 μm thick n-type GaN layer were grown at

1040 °C. These n-type GaN barriers in the one side of QW were step doped with Si atoms by varying the SiH_4 flow rate for several tens of seconds where the other side of QW were step doped with Mg atoms to formed p++/p+ coupled layers. Then InGaN/GaN QW were subsequently grown at a low temperature of 850 °C.

Fig. 1 show the sample structure schematically where the composition and thickness of its layers are listed in Table 1.

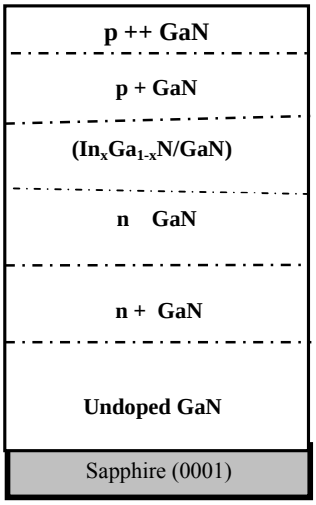

Fig. 1. The schematic diagram of the sample structure.

Table 1. Sample structure

layer	thickness
P+ + GaN	165 µm
P+ GaN	144 Å
$In_{0.055}$ $Ga_{0.945}N$/ GaN	(25 /150) Å
n GaN	15000 Å
n+ GaN	10040 Å
Sapphire (0001)	430 µm

We used in situ X-ray diffraction technique for sample characterization (especially for analyzing of strain and relaxation in their layers). For this purpose, a high resolution X-ray diffraction machine, SEIFERT-3003 was applied for more than 15 hours. The applied X-ray with wavelength of 0.1540nm extracted from copper target and the instrument in the Grazing Incidence Diffraction Geometry Mode was used to measure the thickness and lattice parameters of layers. Therefore for recording the different plans and precise measurement of the c- and a–lattice parameters of GaN barrier we used a double–axis $Cu_{K\alpha 1}$, ɵ-2ɵ scan as shown in Fig. 2.

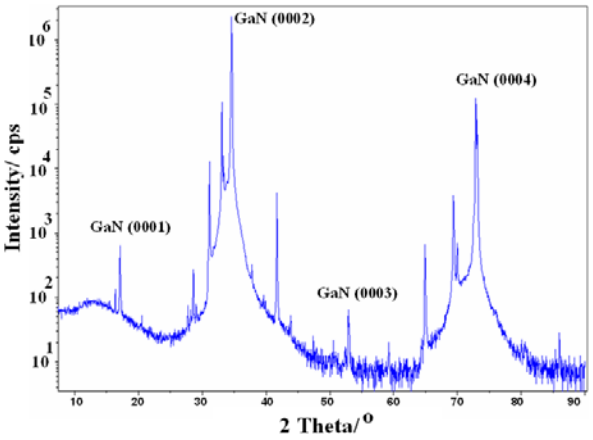

Fig. 2. The in situ XRD spectrum of sample.

We used these parameters for calculation of the strength of internal electric fields. As it explains in the appendix, we find the strength of internal electric fields in the well are about 0.65 MV/cm where the Indium mole fraction to be about %5. For determination of transition energy between sub-bands we used the photoluminescence measurements on $In_{0.05}Ga_{0.95}N$/GaN QW at different temperatures.

For optical characterization of the sample we performed the PL measurements by a Cary Eclipse fluorescence spectrometer and we used a CW 250nm xenon laser for optical excitation. The PL signal was dispersed by a single-grating monochromatic and detected by a UV enhanced liquid nitrogen cooled CCD camera. The sample was placed in a variable temperature cryostat for measurement at 18-300 K. We performed the PL measurements mainly at experimental conditions listed in Table 2.

Table 2. Experimental conditions in PL measurements.

Data mode	Fluorescence
Scan mode	Emission
X Mode	Wavelength (nm)
Start	300.00 (nm)
Stop	600.00 (nm)
Ex. Wavelength	250.00 (nm)
Ex. Slit	5(nm)
Em. Slit	5(nm)
Scan rate	600.00 (nm/min)
Data interval	1.0000(nm)
Averaging Time	0.1000(s)
Excitation filter	250 - 395 nm

In the photoluminescence spectrum displayed in Figure 3, two sets of peaks are visible, whereby the intensity in the second set is lower than that in the first set. The second set corresponds to the transition energy in the well whereas the first set is corresponding to the transition energy in the GaN barrier. Generally, in this quantum well

structure, the transition from the first electron level to the first heavy hole level (i.e., 1e-1hh) is dominant in the PL spectra. Thereafter, two sets of peaks in the PL spectrum (see Fig. 3) are assigned to the 1e-1hh transitions in the barrier and the well, respectively.

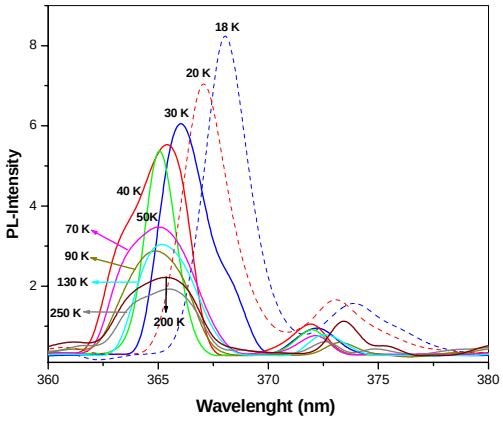

Fig. 3. The photoluminescence spectrum of sample in different temperatures.

3. Self-consistent calculations

In the effective mass approximation, the electronic sub-band states in the growth direction of heterojunctions are solutions for the Schrödinger equation:

$$\frac{-\hbar^2}{2}\frac{d}{dz}\left[\frac{1}{m^*}\frac{d\psi(z)}{dz}\right]+V\psi(z)=E\psi(z) \qquad (1)$$

where m*, V(z), E_i are the carrier effective mass, the potential energy and the energy of the i-th sub-band in the quantum well, respectively. By ignoring the conduction and valence band non–portability, we assume that m* is independent of carrier energy and has an isotropic value changing abruptly at the InGaN/GaN interface. We consider $0.2m_0$ and $1.1m_0$ for electron and hole effective masses in their bulk modulus, respectively where they have well width dependence in QW [13].
The potential term, V(z) in the Schrödinger equation can be assumed as:

$$V(z) = V_c(z)+ V_H(z)+ V_{xc}(z) \qquad (2)$$

$V_c(z)$ represents the conduction–band offset, $V_H(z)$ is the Hartree potential of the electrostatic interaction due to mobile and immobile charges distributed in the system, and $V_{xc}(z)$ is the exchange–correlation potential representing the many–body interaction not included in the $V_H(z)$.
$V_H(z)$ can be obtained by solution of the Poisson equation:

$$\frac{d^2V_H(z)}{dz^2}=\frac{-\rho(z)}{k} \qquad (3)$$

Where k is the dielectric constant and $\rho(z)$ is the density of total charges in the quantum well:

$$\rho(z)=\sigma(z)-n(z)-N_A^-+p(z)+N_d^+(z) \qquad (4)$$

Where σ (z), n(z), $N_A^-(z)$, p(z) and $N_d^+(z)$ denote the density of immobile polarization charges in the GaN/InGaN interface, the density of free electrons in the wells, the density of ionized acceptors in the n-type layer, the density of free holes and the density of Ionized donors in the p-type layer, respectively. Here the n(z) can be obtained by:

$$n(z)=\sum_i n_i|\psi_i(z)|^2 \qquad (5)$$

Where n_i is the density of electrons in the i-the sub-band can be obtained by formula:

$$n_i=\frac{m^*k_BT}{\pi\hbar^2}\ln\left[1+\exp\left(\frac{E_F-E_i}{k_BT}\right)\right] \qquad (6)$$

In a similar manner, the density of holes can be derived from a set of these equations.
As expressed by the equation (6), it is expected that the n(z) will have different values at various temperatures. Obviously for neutrality conditions the following relation must be satisfied:

$$\int\rho(z)dz=0 \qquad (7)$$

In order to obtain $V_{xc}(z)$, we applied the density functional theory using a simple approximation called Local Density Approximation (LDA). In this approximation $V_{xc}(z)$ can be parameterized in an analytic form[14] such that:

$$V_{xc}(z)=-\left[1+\frac{0.7734r_s}{21}\ln\left(1+\frac{21}{r_s}\right)\right]\frac{2E_R}{\pi\alpha r_s} \qquad (8)$$

Where $\alpha=(4/9\pi)^{1/3}$ and r_s is the radius of a sphere containing one electron:

$$r_s=\left[\frac{4}{3}\pi a^{*3}n(z)\right]^{-1/3} \qquad (9)$$

In the unit of the effective Bohr radius the effective Rydberg energy is given by:

$$E_R=\frac{e^2}{8\pi ka^*} \qquad (10)$$

V_{xc} gives a significant effect on the electron sub-band states and band gap with an increase of electrons density [15].

In this way, we solved the Schrödinger equation and Poisson equation iteratively until a self-consistency was achieved taking into account the Hartree and Exchange–correlation potential. Fig. 4 depicts the model calculations for conduction band profile based on the lowest three wave functions in $In_{0.05}Ga_{0.95}N$/GaN QW sample. In this

calculation, a barrier width of 150 Å and well depth of 25 Å were assumed for GaN and InGaN, respectively. The carrier density in the well is thus determined.

Also we determined the density of carriers in the well based on this calculation. Fig. 5 displays the temperature dependence of electrons concentration of the $In_{0.05}Ga_{0.95}N$/GaN QW sample. We notice to large values and linear dependence for electrons density in the step-doped sample where they have nonlinear variations with smaller values in the other samples.

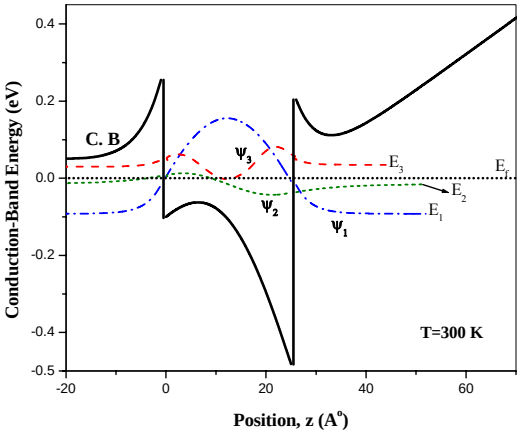

Fig.4.The Conduction band profile of a step doped model InGaN/GaN Quantum Well. We assumed the GaN (barrier) width=150 Å, Well (InGaN) width=25 Å

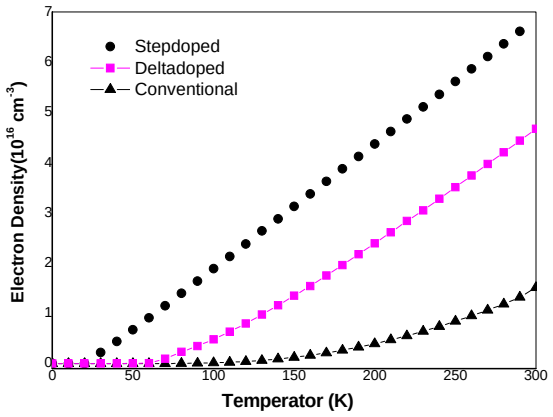

Fig.5. Theoretical results for temperature dependence of electron concentration in three $In_{0.05}Ga_{0.95}N$/GaN QW structures.

It is well known that when an epitaxial layer is coherently grown on a mismatched lattice layer, it can be subjected to strain and consequently, piezoelectric polarization prevails in these layers. For calculating the strength of strain and related piezoelectric field in the sample (explained in the appendix), we used lattice constants measurement by X-ray diffraction technique. It is noticeable that the sample under study is influenced by biaxial strain perpendicular to [0001]. As mentioned before, the presence of this biaxial strain causes piezoelectric polarization in these layers thus; its related electric field has considerable effect on the band offset and the intersubband transitions, as red-shift in optical transitions we see in the main part of PL spectra [16, 17]. Therefore, the strength of internal electric field is determined and then added to the related main potential term (Eq. 3) for the evaluation of inter-subband transition energy. We evaluated of inter-subband transition energy with and without considering internal electric field. We found that there is an acceptable agreement between theoretical result and experimental data where we didn't consider internal electric field as depicted in Figure 6. However there is some mismatch between exp. Data (filled squres) and theoretical results at low temperatures that is attributed to the localization of carriers in the fluctuations of potential in the active layer[18].

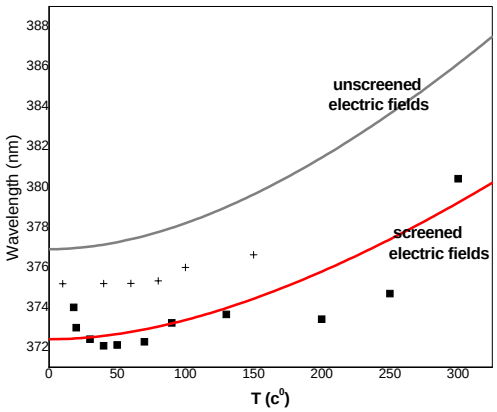

Fig.6. The peak position of PL spectrum in the InGaN/GaN Quantum well at different temperatures. The filled squares represent the measured PL peaks in our sample where the solid lines represent the calculated values with and without considering internal electric fields, respectively. The crossed (+) symbols represent the measured PL peak position in delta doped sample [9].

4. Conclusion

In summary, we have studied the influence of step doped GaN barriers (p++/p+ and n/n+) on optical property of InGaN/GaN QW, especially on their intersubband transitions. The strong screening of free electrons originated from GaN barriers significantly reduced QCSE. this reduction caueses a strong blue shifted in PL spectrum compare to conventional InGaN/GaN QW structures where a weaker one for delta doped InGaN/GaN QW structures is reported in other publications.

in theory, we presented a self-consistent numerical method can be used for calculation of conduction band profile and subbands structure of InGaN/GaN QWs. In special case we used this calculation method for $In_{0.05}Ga_{0.95}N$/GaN QW with two couple step doped layers around its active region. The internal electric fields, the

Hartree interaction and the exchange–correlation (representing the many–body interaction) were dominant in the potential term. We found in any case the carrier's concentration and transition energy is sensitive to doping concentration, the GaN barriers width and to temperature performance. The calculated results for transition energy are compatible with corresponding experimental data obtained from PL measurements especially, in low temperatures and in room temperature.

Acknowledgment

The authors would like to thanks Islamic Azad University, Varamin-Pishva Branch, for financial support of this research work. Also they would like to thank Professor Dimitris Pavlidis and co-workers from Dept. of Microelectronic Engineering and Dr. Jörg Zimmerman of the Dept. of Material Science (Electronic Materials Division-Darmstadt University of technology) for their technical assistances and valuable discussions.

Appendix: Details on internal electric fields calculations for sample

The relationship between piezoelectric polarization and strain in the case of a wurtzite structure is given by [14]:

$$\begin{bmatrix} p_x \\ p_y \\ p_z \end{bmatrix} = \begin{bmatrix} 0 & 0 & 0 & 0 & e_{15} & 0 \\ 0 & 0 & 0 & e_{24} & 0 & 0 \\ e_{13} & e_{23} & e_{33} & 0 & 0 & 0 \end{bmatrix} \begin{bmatrix} \varepsilon_{xx} \\ \varepsilon_{yy} \\ \varepsilon_{zz} \\ \varepsilon_{yz} \\ \varepsilon_{zx} \\ \varepsilon_{xy} \end{bmatrix} \quad (11)$$

where P_i, e_{ij} and ε_{ij} are the components of electric polarization vector, the elements of piezoelectric tensor and the components of strain vector in the strained layer, respectively, and z direction is set parallel to the [0001] axis. The strain elements in the case of a wurtzite structure are:

$$\varepsilon_{yz} = \varepsilon_{zx} = \varepsilon_{xy} = 0$$
$$\varepsilon_{zz} = -\frac{2C_{13}}{C_{33}}.\varepsilon_{xx} \quad (12)$$
$$\varepsilon_{xx} = \varepsilon_{yy} = \frac{a_s - a_e}{a_s}$$

Where α_e, α_σ and $\chi_{\iota\varphi}$ are the free-standing α-axis lattice constants of the epitaxial layer (InGaN) and the substrate (GaN), and the elastic stiffness constant for the epitaxial layer, respectively.

In order to calculate the magnitude of stress in our sample we need to know about the structure and the lattice constants of layers then we used XRD spectroscopy for this purpose shown in Fig. 2. As it is clear there are two intensive peaks at 34.61º and 72.91º due to (0002) and (0004) planes, respectively also a weak one at 32.40º due to (1000) plane which are known the characteristic planes for a crystal with hexagonal structure. By using these experimental evidences we found lattice parameters can be evaluated from following relation in hexagonal phase structures [19]:

$$\frac{2\sin\theta}{\lambda} = \sqrt{\frac{4}{3}\frac{h^2+hk+k^2}{a^2} + \frac{l^2}{c^2}} \quad (13)$$

By considering the carrier mentioned in Ref. [6] we found that the sample suffers a considerable biaxial compressive strain and consequently piezoelectric and spontaneous polarization which their variations in different In mole fractions depicted in Fig. 7.

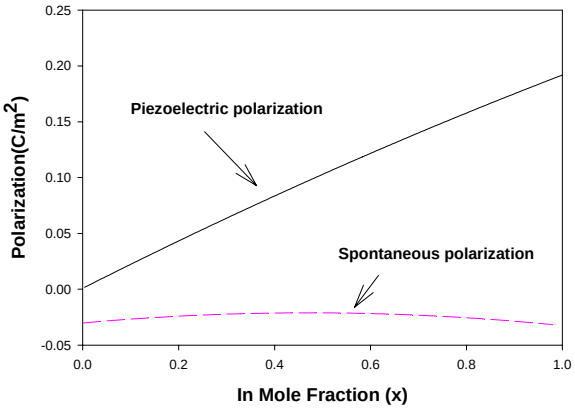

Fig. 7. The piezoelectric and spontaneous polarization in the InGaN/GaN QWs with different indium mole fractions.

These results can be used to determine the basal plane strain and stress in these layers. By using the values of material parameters in wurtzite InGaN reported in Ref. [20] we calculated the real-time polarization on the InGaN Qw:

$$P_{SP}(x) = x(-0.032) + (1-x)(-0.029) + bx(1-x) \quad (14)$$

Where the bowing parameter (b) used for this material is about 0.037 [21].

Figure 7 shows the calculated piezoelectric and real-time polarization in these structures.

The electric field along [0001] in the strained layer due to piezoelectric effect is given by:

$$E_z(x) = \frac{p_z(x)}{K\varepsilon_o} \quad (15)$$

Where K and ε_o are the dielectric constants of the material and permittivity of the free space respectively.

References

[1] S. Nakamura and G. Fasol, "The Blue Lasers Diode", Springer, Berlin p. 1, 1997.
[2] F. A. Poce, D.P. Bour, Nature, **368**, 351 (1997).
[3] R. Sharma, P. M. Pattison, et al, J. Appl. Phys. Lett. **87**, 231110 (2005).
[4] J. M. Wagner, F. Bechstedt, Phycal. Review B. **66**, 115202 (2002).
[5] John H. Davies,The physics of low-dimensional semiconductors, Cambridge university press, 258, 1998.
[6] H. R. Alaei, H. Eshghi, R. Riedel, D. Pavlidis, Chinese journal of physics. **48**, 400 (2010).
[7] Stephan Figge, Tim Bottcher, Detlef Homme, Christoph Zellweger, Marc Ilegem, phys. stat. sol. (a). **200**(1), 83 (2003).
[8] M. K. Kwon, I. K. Park, S. Baek, J. Kim, S. Parka, J. Appl. Phys. **97**, 106109 (2005).
[9] M. Kwon, I. K. Park, J. Y. Kim, J. Kim, S. B. Seo, S. Parkc, J. Appl. Phys. **102**, 073115 (2007).
[10] I. H. Tan, G. L. Snider, L. D. Chang and E. L. H, J. Appl. Phys. **66**, 4071 (1990).
[11] M. B. Patil, U. Ravaioli, Solid State Electronics. **33**(7), 593 (1990).
[12] K. S. Lee, D. H. Yoon, S. B. Bae, M. R. Park, G. H. Kim, ETRI journal. **24**(4), 270 (2002).
[13] H. R. Alaei, H. Eshghi, phys. Lett. A. **374**, 66 (2009).
[14] L. Hedin, B. I. Lundqvist, J. Phys. C. **4**, 2064 (1971).
[15] F. Stern , S. D. Sarma, Phys. Rev. B, **30**(2) 840 (1984).
[16] T. Takeuchi, S. Sota, M. Katsuragawa, M. Komori, H. Takeuchi, H. Amano, I. Akasaki, Jpn. J. Appl. Phys. **36**, 382 (1997).
[17] R. Tao, T. Yu, C. Jia, Z. Chen, Z. Qin, G. Zhang, phys. Status Solidi A. **206**(2), 206 (2009).
[18] E. Abdoli, H. Haratizadeh, phys. Status Solidi B. **247(**1) 170 (20109).
[19] M. Birkholz, "Thin Film Analysis by X-Ray Scattering", WILEY-VCH Verlag p. 11, 2006.
[20] F. Bernardini, V. Fiorentini, D.Vanderbilt, Phys. Rev. B. 63 (2001) 193201.
[21] H. Morkoç,"Nitride Semiconductors and Devices", Springer-Verlag, 1999.

*Corresponding author: hr_alaei@yahoo.com